Available online at www.sciencedirect.com
ScienceDirect
Journal of Chromatography B, 850 (2007) 499–506
JOURNAL OF CHROMATOGRAPHY B
www.elsevier.com/locate/chromb

Conjugation of enzyme on superparamagnetic nanogels covered with carboxyl groups

Jun Hong [a,b], Dongmei Xu [a,b], Peijun Gong [a,b], Hongjuan Ma [a,b], Li Dong [a,b], Side Yao [a,*]

[a] *Shanghai Institute of Applied Physics, Chinese Academy of Sciences, Shanghai 201800, PR China*
[b] *Graduate School of Chinese Academy of Sciences, Beijing 100039, PR China*

Received 30 September 2006; accepted 20 December 2006
Available online 22 January 2007

Abstract

α-Chymotrypsin (CT) as model enzyme was conjugated onto the novel carboxyl-functionalized superparamagnetic nanogels, prepared *via* facile photochemical in situ polymerization, by using 1-ethyl-3-(3-dimethylaminepropyl) carbodiimide (EDC) as coupling reagent. The obtained magnetic immobilized enzyme was characterized by use of photo correlation spectroscopy (PCS), Fourier transform infrared spectroscopy (FT-IR), X-ray diffraction (XRD) measurement, thermogravimetric (TG) analysis and vibrating sample magnetometer (VSM) measurement. PCS result showed that the immobilized enzyme was 68 nm in diameter while the magnetic nanogels with carboxyl groups were only 38 nm; enzyme immobilization led to pronounced change in size. Superparamagnetic properties were retained for Fe_3O_4 after enzyme immobilization while slightly reducing its value of saturation magnetization. Immobilization and surface coating did not induce phase change of Fe_3O_4 by XRD analysis. The binding capacity was 30 mg enzyme/g and 37.5 mg enzyme/g nanogel determined by TG analysis and BCA protein assay, respectively. Specific activity of the immobilized CT was calculated to be 0.77 U/(mg min), 82.7% as that of the free form.

Keywords: Carboxyl-functionalized magnetic nanogels; Immobilized enzyme; Magnetic separation; Photochemical in situ polymerization

1. Introduction

Enzymes are commonly preferred to chemical catalysts because they are more selective, produce a cleaner product and achieved higher yield, in biological applications. The main benefit from immobilized enzymes is that they can be retrieved after use, minimizing complex pollution. Enzyme immobilization provides a preferable approach to ease enzyme reuse and to extend its half-life.

The success of an immobilized enzyme for practical applications is strongly dependent on the properties of the carriers employed. The carrier should have a high capacity for enzyme immobilization. Carriers should also be chemically stable and should provide a prolonged life of activity for immobilized enzyme system.

In recent years, a large variety of nano-sized carriers, which might be organic or inorganic in nature, have been used in the attachment of enzymes [1–6]. Enzyme activity and stability are maximized with smaller particle supports. However, recovery of small immobilized enzyme particles from reaction system remains difficult using conventional separation techniques. In view of these, magnetic microbeads have become increasingly attractive [7–12]. The use of magnetic microbeads as supports for enzyme immobilization is mainly based on the magnetic feature of the solid-phase that enables to achieve a rapid separation in a magnetic field, as well as the capital and operation costs [13,14]. Nowadays, functional magnetic microbeads could be produced in a number of ways [15–17] but usually involved the coating of magnetically susceptible particles with synthetic polymers having reactive sites for the affinity ligand attachment.

Magnetic nanogels, a class of inorganic/polymer core-shell composites with nano-scaled dimension, are composed of a core of magnetically susceptive nanoparticle and a shell of cross-linked polymer network. They usually possess excellent swollen capacity and hydrophilicity, and thereby can be widely used as carriers in biotechnological applications such as enzyme immobilization and targeted drug system.

On the investigation of the photo-polymerization process of vinyl monomers in several solvents, Hoffman et al. [18] and Stroyuk et al. [19] found out that quantum-sized semiconductor

* Corresponding author. Tel.: +86 2159554681; fax: +86 2159554681.
E-mail address: yaoside@sinap.ac.cn (S. Yao).

1570-0232/$ – see front matter © 2007 Elsevier B.V. All rights reserved.
doi:10.1016/j.jchromb.2006.12.035

particles were efficient photoinitiators to initiate polymerization of monomers in high quantum yields. Theoretically, it was possible to prepare core-shell magnetic nanogels *via* photochemical method using quantum-sized Fe_3O_4 nanoparticles as photoinitiator. Actually, magnetic nanogels with amino groups or hydroxyl groups had been successfully prepared by photochemical in situ polymerization in our group and the possible mechanism was proposed [20,21]. The surface of the synthesized magnetic nanogels remained reactive and could be available for post synthesis chemical modification. More important, it was convenient to manipulate properties (including particle size, polymeric extent and surface charge) of the synthesized nanogels by varying the experimental factors, i.e. irradiation time, irradiation intensity and monomer concentration. In this sense, photochemical in situ polymerization represented a facile method in fabrication of magnetic nanogels in a wide variety of compositions.

The aim of the present work was to provide a novel and facile route to prepare functional magnetically susceptive support with a size of several nanometers for enzyme immobilization. α-Chymotrypsin (CT) as model enzyme was anchored to the carboxyl-functionalized magnetic nanogels by 1-ethyl-3-(3-dimethylaminepropyl) carbodiimide (EDC) and *N*-hydroxysuccinimide (NHS) at room temperature. The resultant immobilized enzyme was characterized by photo correlation spectroscopy (PCS), FT-IR spectroscopy, X-ray diffraction (XRD) measurement, thermogravimetric (TG) analysis and vibrating sample magnetometer (VSM) measurement, etc. Several properties for the immobilized CT were evaluated.

2. Experimental

2.1. Materials

Methylacrylic acid (MAA), *N*-benzoyl-L-tyrosine ethyl ester (BTEE), *N*,*N*′-Methylene-bis-(acrylamide) (MBA), ethanol amine, carbodiimide hydrochloride (EDC·HCl) and *N*-hydroxysuccinimide were all of analytic grade and purchased from Shanghai Chemical Reagents Corp. α-Chymotrypsin and BCA protein assay kit were available from commercial source. Fe_3O_4 nanoparticles with hydrodynamic diameter of 10 nm were synthesized by partial reduction method [22]. The water used in the experiment was triply distilled. MAA and MBA were purified prior to use.

2.2. Synthesis of carboxyl-functionalized magnetic nanogels

0.5 ml of MAA and 1 ml of 1% MBA were mixed well in 120 ml of water, and adjusted pH to 6 with 5 M NaOH before charging into the quartz flask. The reaction system was bubbling nitrogen gas for 10 min to exclude the air inside the flask. 20 mg of Fe_3O_4 nanoparticles was dropped into the flask, then turning on the xenon lamp equipment and irradiating for 30 min. Nitrogen gas was bubbled as protective gas throughout the experiment. The obtained magnetic nanogels were magnetically recovered once the reaction completed, and washed several times with water.

2.3. Enzyme immobilization

EDC·HCl (5 mg) and NHS (7 mg) were dissolved in 3 ml of phosphate buffer solution (50 mM, pH 6.5). 20 mg of carboxyl-functionalized magnetic nanogels was added into the mixture above. The reaction was carried out at water bath of 0 °C for 30 min. After completion of the reaction, the magnetic nanogels was gathered by a magnet and washed with PBS (50 mM, pH 6.5). The concentrated magnetic nanogels were redispersed in 3 ml of PBS (50 mM, pH 6.5), and then 5 mg of CT was introduced into the immobilization medium. The mixture was shaken for 24 h at room temperature. After reaction completed, the immobilized enzyme was magnetically recovered and washed several times with PBS (50 mM, pH 6.5) until no free enzyme detected in the washing solution. The washing solution was pooled for protein assay. Subsequently, 1 ml of 10 mM ethanolamine was added into the resultant immobilized enzyme, and the reaction was kept for 1 h at room temperature. Finally, the immobilized enzyme was separated by a magnet and redispersed in pH 3 of hydrochloric acid for further measurements.

The amount of CT immobilization on the carboxyl-functionalized magnetic nanogels was determined by measuring the enzyme concentration in the washing solution, using BCA protein assay [5]. A calibration curve constructed with BSA was used in the determination of enzyme in the washing solution. The binding capacity was calculated according to the following formula:

$$M\left(\frac{\text{mg enzyme}}{\text{g nanogel}}\right) = \frac{(m - C_1 V_1)}{W}$$

where M represented the binding capacity, m the amount of enzyme introduced into the immobilization medium, C_1 and V_1 the enzyme concentration and volume of the washing solution, respectively, W the weight of the magnetic nanogel.

2.4. Characterization

Size distributions of the carboxyl-functionalized magnetic nanogels and immobilized CT were carried out on a laser analyzer for particle size (Mastersizer 3000, Malvern), which provided a Gauss curve concerning the distribution of nanoparticles (percentage abundance versus diameter). The morphology was investigated with a PHILIPS CM120 transmission electron microscopy (TEM) with an accelerated voltage of 80 kV. The samples for TEM measurements were prepared by placing one or two drops of suspension onto a carbon stabilized copper grid (200 mesh) and freeze drying (liquid nitrogen, −196 °C) it. Fourier transform infrared (FT-IR) spectra from the KBr pellet with samples were recorded on a Nicolet FT-IR spectrophotometer in a wave number ranging from 4000 to 400 cm^{-1} with a resolution accuracy of 4 cm^{-1}. The crystalline phases of the carboxyl-functionalized magnetic nanogels and immobilized enzyme were identified by use of a Philips X-ray diffractometer (Cu Kα radiation, λ = 1.5418 Å). Magnetization measurements were obtained at room temperature in magnetic fields up to 10 k Oe using a vibrating sample magnetometer (Princeton Applied Research, model 155). Thermogravimetric

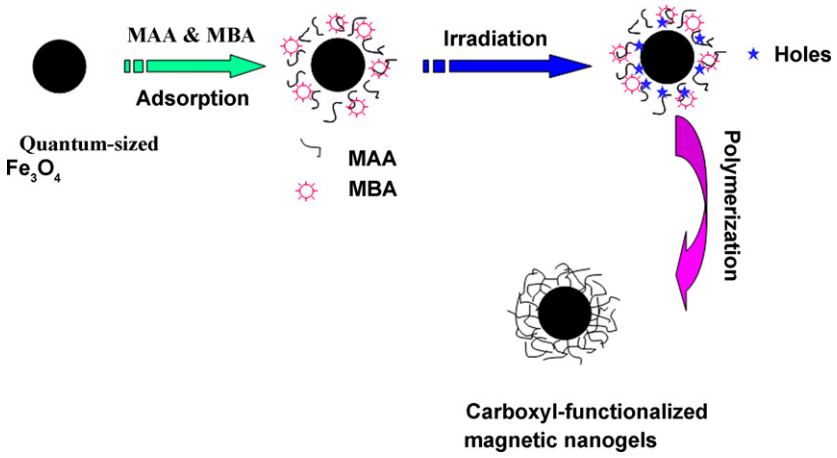

Fig. 1. Synthesis scheme of carboxyl-functionalized magnetic nanogels by photochemical in situ polymerization.

analysis was estimated by a simultaneous DTA-TG and DSC apparatus (Shimadzu, Japan) by heating the samples from room temperature to 700 °C under N_2 atmosphere at a heating rate of 10 °C min^{-1}.

2.5. Activity assay of the immobilized enzyme

Unit of enzyme activity (U) was defined as: 1 mg of protein will hydrolyze 1.0 μmol of BTEE per minute at pH 7.8 at 25 °C.

Activity of the immobilized CT was determined by a UV–vis spectrophotometer (Shimadzu, Model 1601; Tokyo, Japan):

$$\text{BTEE} + \text{H}_2\text{O} \xrightarrow{\text{CT}} N - \text{benzoyl} - \text{L} - \text{tyrosine} + \text{ethanol}$$

The assay mixture consisted of 1.42 ml of Tris–HCl buffer (80 mM, pH 7.8), 1.4 ml of 1.18 mM BTEE and 0.08 ml of 2 M $CaCl_2$). After addition of 0.1 ml of enzyme solution, the reaction was carried out at 25 °C for 3 min. The suspension was immediately separated by an external magnetic field of 0.5 T and measured the absorbance of the solution at 256 nm. Specific activity was estimated using the following formula:

$$\text{Specific activity (U/(mg}\,min)) = \frac{\Delta A}{0.964 \times \text{Ew} \times 3 \times 3}$$

where ΔA was the absorbance of the solution at 256 nm, Ew denoted the amount of enzyme in 0.1 ml of enzyme solution, 0.964 was the molar extinction coefficient of *N*-benzoyl-L-tyrosine at 256 nm.

3. Results and discussion

3.1. Synthesis of the carboxyl-functionalized magnetic nanogels

The carboxyl-functionalized magnetic nanogels were prepared from MBA, MAA and Fe_3O_4 nanoparticles *via* photochemical in situ polymerization [23]. The synthesis scheme was presented in Fig. 1.

In the experiment, a 500 W xenon lamp, whose irradiation spectrum was consecutive, was used as irradiation source. MAA instead of acrylic acid was chosen as coating agent because of higher reactivity when exposure to UV light. Fe_3O_4 nanoparticles were served as photoinitiator to initiate MAA coating on their surface, as well as core of the magnetic nanogels. As MAA tended to homo-polymerize due to self-assembly when exposure to UV light, and enhanced viscosity of the reaction system. In this case, it was difficult to isolate the synthesized magnetic nanogels from the reaction medium. Therefore, pH of the reaction medium was adjusted with 5 M sodium hydroxide solution. After pH adjusting, part of carboxyl groups was converted to carboxylate, self-assembly was destroyed by electrostatic repulsive force between carboxylates, and hence homo-polymerization of MAA was effectively depressed. Meanwhile, amount of MAA coating on the surface of Fe_3O_4 increased.

The amount of MAA coating on the surface of the Fe_3O_4 nanoparticles could be manipulated by changing the irradiation time, irradiation intensity and monomer concentration, etc. Nevertheless, there was a paradox between polymeric extent and particle size; higher polymeric extent would result in larger particle size. In fact, suitable amount of MAA was necessarily required in order to yield higher binding capacity for enzyme immobilization. Accordingly, a balance should be kept between polymeric extent and particle size.

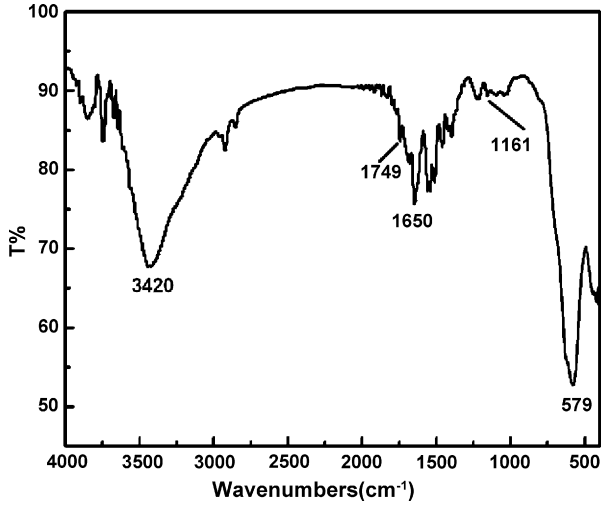

Fig. 2. FT-IR spectrum of carboxyl-functionalized magnetic nanogels.

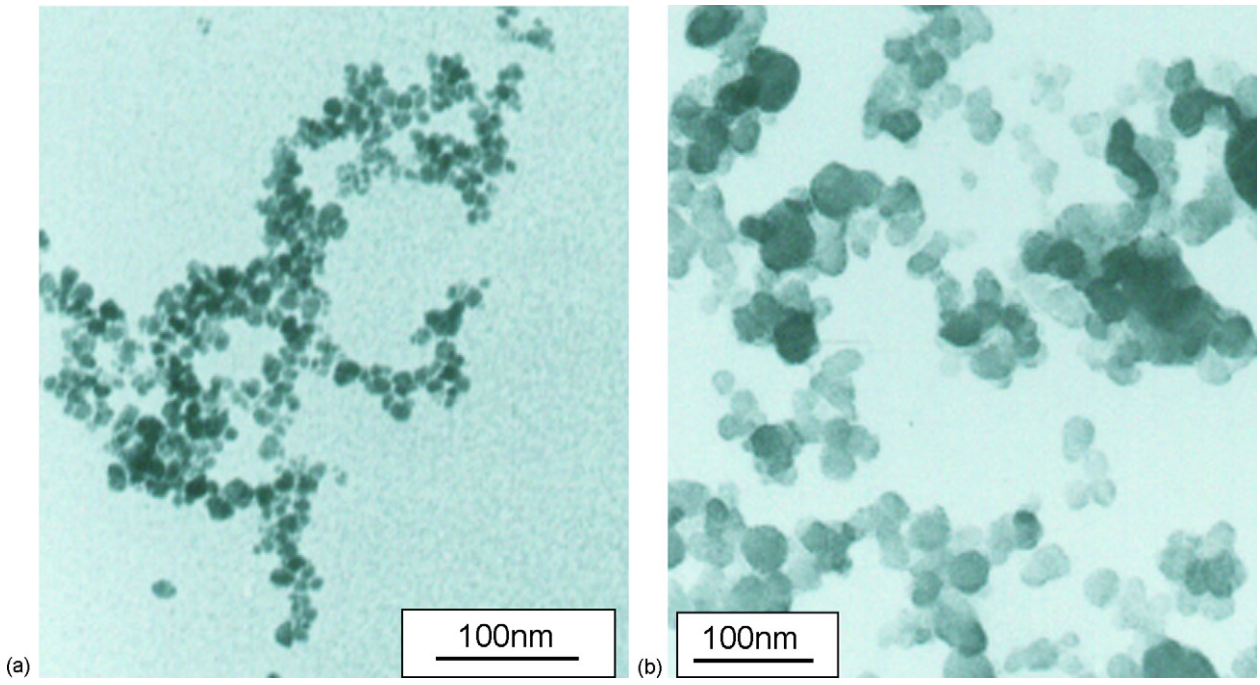

Fig. 3. TEM images of (a) carboxyl-functionalized magnetic nanogels and (b) immobilized CT.

3.2. Characterization of superparamagentic nanogels covered with carboxyl groups

FT-IR spectrum of the poly(MAA)-coated Fe_3O_4 nanoparticles was presented in Fig. 2. The presence of Fe_3O_4 core could be seen by the strong absorption band around 579 cm^{-1}, which corresponded to the Fe–O bond of naked Fe_3O_4. The bands of 1749 cm^{-1} and 1161 cm^{-1}, were assigned to the C=O and C–O stretching vibrations of carbonyl group [24]. The band of 1650 cm^{-1} was attributed to the C=O stretching vibrations of carbonyl group of MBA, which served as cross-linker in the fabrication. Moreover, the wide band of 3600–3300 cm^{-1} corresponded to the O–H stretching vibration of MAA and a trace amount of water. The results above confirmed that MAA was coated on the surface of Fe_3O_4 successfully. Nevertheless, the relative intensity of the characteristic peaks of carbonyl group was comparatively low in the FT-IR spectrum (see Fig. 2). It might be related to the small amount of MAA coated on the surface of Fe_3O_4, as a result of the reaction medium pH adjusting with sodium hydroxide and smaller polymeric extent of MAA coating on the surface of Fe_3O_4 nanoparticles. On the other hand, it was accepted that characteristic peaks of carbonyl group disappeared (actually shifted) when carboxyl groups was converted to carboxylate. The two factors above made relative intensity of the bands of 1749 cm^{-1} and 1161 cm^{-1} weak.

The carboxyl-functionalized magnetic nanogels with a particle size of 20 ± 3 nm was close to spherical, core-shell structure could be clearly obtained from its TEM image (Fig. 3a). However, the average size was determined to be 38 nm by PCS (Fig. 4). The marked difference in particle size of nanoparticles, determined by TEM or PCS, was caused by method itself. PCS was usually used in determination of hydrodynamic diameter of nanoparticles while TEM was a tool for evaluating particle size in dried state. Particle size from PCS was undoubtedly larger than that of TEM measurement because of the hydrated layer. As shown in Fig. 5, no hysteresis loop was observed, with both coercivity and remanence close to zero, suggesting that the magnetic nanogels were superparamagnetic. Saturation magnetization of the magnetic nanogels was found to be 62.8 emu/g. With such high magnetization value, the obtained magnetic nanogels could be easily isolated by a common magnet. The TG analysis was carried out to estimate the polymeric extent of the synthesized magnetic nanogels. As presented in Fig. 6a, a weight loss of 0.9% was observed when the temperature up to 120 °C. This indicated that a trace amount of water (including bound water) was contained in the dried magnetic nanogels. Another 3.3%

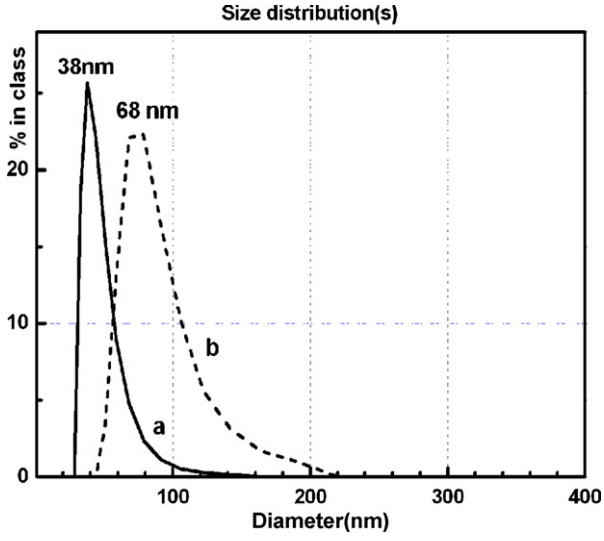

Fig. 4. Size distributions of (a) carboxyl-functionalized magnetic nanogels and (b) immobilized CT measured by PCS.

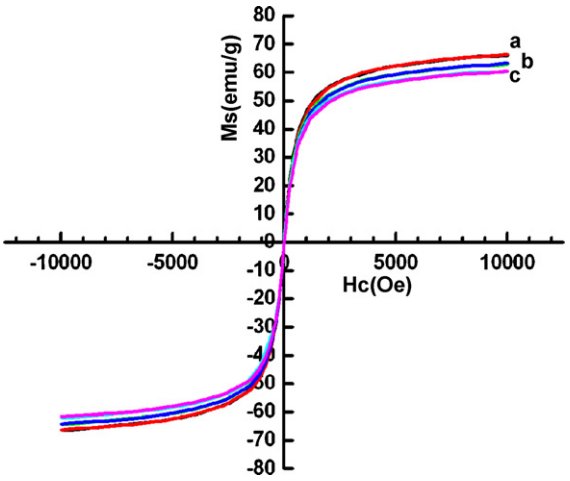

Fig. 5. Hysteresis loops of (a) freshly prepared Fe_3O_4; (b) carboxyl-functionalized magnetic nanogels; and (c) immobilized CT measured at room temperature.

weight loss occurred when the temperature ranging from 120 °C to 520 °C due to polymer decomposition under nitrogen atmosphere, namely, polymeric extent of the carboxyl-functionalized magnetic nanogels was determined to be 3.3% by TG analysis (Fig. 6a). Magnetic content of Fe_3O_4 was higher than 90%. To our knowledge, magnetic microspheres with such high magnetite content had not been prepared by other method reported.

3.3. Immobilization of CT onto the carboxyl-functionalized magnetic nanogels

CT was covalently bound to the carboxyl-functionalized magnetic nanogels by using EDC as coupling reagent [25]. The immobilization protocol was demonstrated in Fig. 7. Firstly, carboxyl groups existing on the nanogels reacted with NHS in the presence of EDC, and resulted in the formation of active ester. Then, CT was attached onto the magnetic nanogels *via* the resultant active ester.

It deserved to mention that pH played an important role in the enzyme immobilization. For extreme situation (inadequate pH value or long term exposure to medium of inadequate pH), enzymes would permanently loss their activities. On the other hand, extreme acidic or basic immobilization medium would accelerate hydrolysis of active ester groups. In view of these, neutral or slightly acidic pH was chosen as the pH of the immobilization medium in the experiment. The amount of CT immobilization onto the support was dependent on the amount of the reactive groups available for enzyme immobilization, immobilization pH, immobilization time and ratio of enzyme to the functional magnetic nanogels, etc. After completion of enzyme immobilization, the unreacted active ester on the immobilized enzyme should be treated with ethanolamine, otherwise the immobilized enzymes would be linked *via* the unreacted active ester and led to serious aggregation.

The proof immobilization of CT onto the magnetic nanogels covered by carboxyl groups was confirmed by FT-IR measurement. As shown in Fig. 8, strong absorption band at 579 cm^{-1} was assigned to the Fe–O bond of naked Fe_3O_4. The peaks occurred at 1637 cm^{-1}, 1530 cm^{-1} and 1399 cm^{-1}, which were characteristic peaks of free CT, were also observed in the spectrum of immobilized enzyme. However, the intensities of the peaks were weak in comparison to free CT. This might be due to the small amount of enzyme immobilized on the magnetic nanogels. Additionally, it should be noted that the immobilized enzyme was washed several times with PBS to minimize free enzyme adsorption by the magnetic nanogels. Accordingly, we could conclude that CT was covalently immobilized onto the carboxyl-functionalized magnetic nanogels successfully.

3.4. Properties of bound CT

3.4.1. Particle size

As reported, enzyme immobilization would not significantly result in change in size of particles [26]. However, this phenomenon was not observed in present case. As presented in Fig. 4, the immobilized enzyme was measured to be 68 nm while

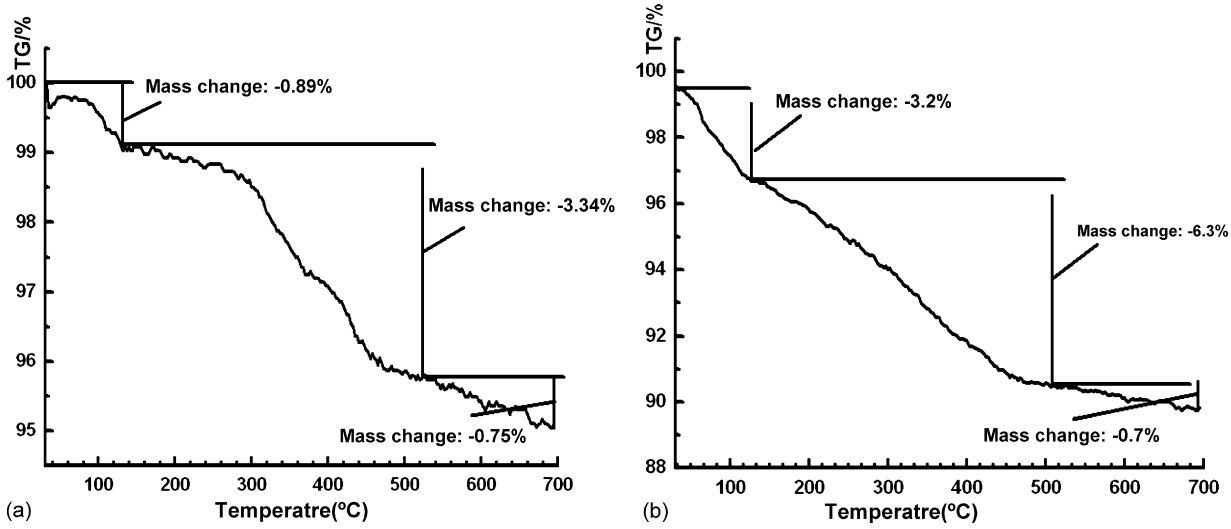

Fig. 6. TG curves of (a) carboxyl-functionalized magnetic nanogels and (b) immobilized CT.

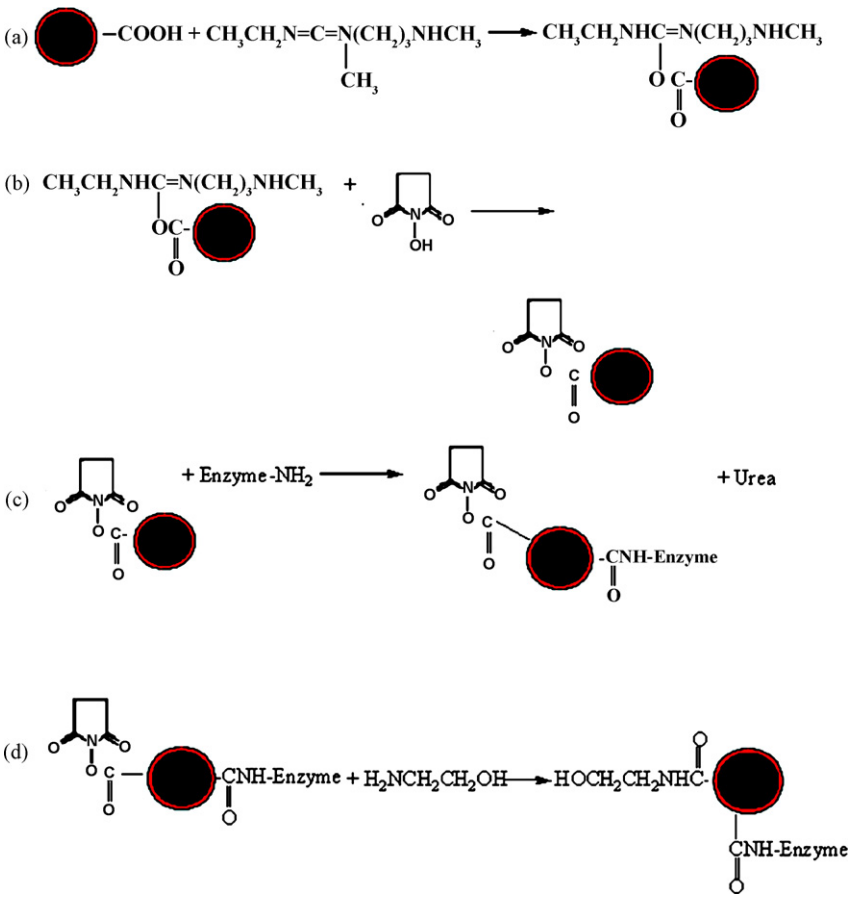

Fig. 7. Schematic representation of enzyme immobilization *via* active ester.

the carrier for immobilization was only 38 nm; marked change in diameter was observed after CT being immobilized onto the magnetic nanogels with carboxyl groups; meanwhile size distribution of the immobilized CT was broader than that of the carboxyl-functionalized magnetic nanogels. The pronounced increase in particle size might result from aggregation of the immobilized enzyme due to magnetic attraction. On the other hand, the linkage between immobilized enzymes *via* the unreacted active ester should be also considered (see Fig. 9). With respect to the broader size distribution, it might be due to the aggregation of the immobilized enzyme.

3.4.2. Morphology

In the experiment, the samples for TEM observation were freeze dried in order to reflect intrinsic morphology of the samples. As was evident from Fig. 3b, serious aggregation was observed for the resultant immobilized enzyme, and it was impossible to recognize single immobilized enzyme particle from its TEM image. The aggregation might be attributed to the magnetic attraction between magnetic particles. Furthermore, salts played an important role in the aggregation of nanoparticles.

3.4.3. Binding capacity

TG analysis was performed to determine the polymeric extent and amount of CT immobilization on the magnetic nanogels. The measurement was carried out under nitrogen atmosphere to minimize mass increase due to oxidation. As shown in Fig. 6b, the weight ratio of coating layer (including poly(MAA) and CT) on the carboxyl-functionalized magnetic nanogels was 6.3%. Apart from the weight ratio of poly(MAA)), CT immobilization on the carboxyl-functionalized magnetic nanogels was determined to be 3.0%, namely, binding capacity was estimated to be 30 mg enzyme/g nanogel by TG analysis.

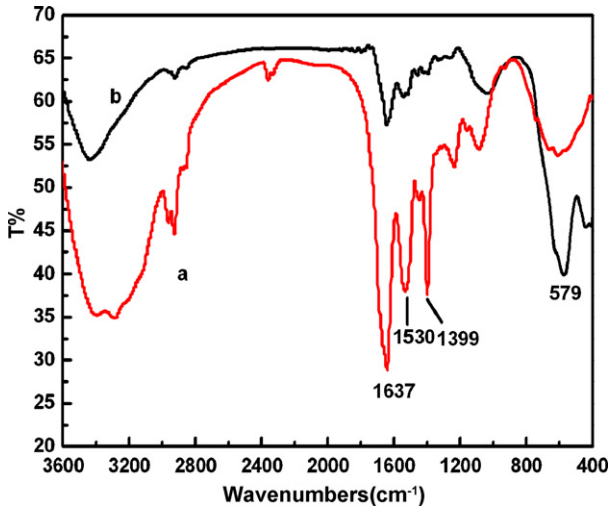

Fig. 8. FT-IR spectra of (a) free CT and (b) immobilized CT.

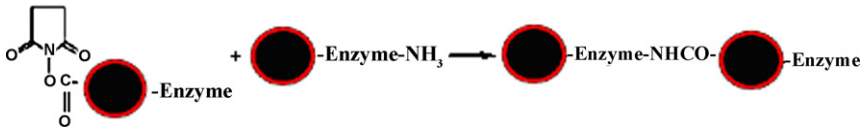

Fig. 9. Linkage between immobilized enzymes *via* active ester.

The binding capacity of the immobilized enzyme was also determined by using BCA protein assay. The binding capacity was estimated to be 37.5 mg enzyme/g nanogel. There was an error of 20% between TG analysis and BCA protein assay. This might be caused by accuracy of the two methods. We usually preferred to the binding capacity determined by BCA protein assay while the result from TG analysis just as reference.

3.4.4. Magnetic properties

Magnetic properties of the immobilized CT were investigated by VSM measurement at room temperature. The resultant immobilized enzyme exhibited excellent response to applied magnetic field, and its saturation magnetization was determined to be 59.6 emu/g (Fig. 5). Taking into account the weight ratio of polymers (including CT and cross-linked poly(MAA)), saturation magnetization of Fe_3O_4 was calculated to be 63.6 emu/g, which was slightly decreased in comparison with that of freshly prepared Fe_3O_4 (66.3 emu/g) for the nonmagnetic layer on the surface of Fe_3O_4, thus affecting the uniformity or magnitude of magnetization due to quenching of surface moments [27]. Another tendency towards lower magnetization might be the oxidation of the surface of magnetite during the polymerization process, which resulted in the formation of a trace amount of maghemite, whose saturation magnetization (76 emu/g) was lower than that of bulk magnetite (92 emu/g). The immeasurable coercivity and remanence indicated that superparamagnetic properties were retained for Fe_3O_4 after immobilization; the superparamagnetic immobilized enzyme could be readily recovered by a magnet. Furthermore, the high magnetic content of Fe_3O_4 (as high as 90%) and strong saturation magnetization (59.6 emu/g) allowed the rapid isolation of immobilized enzyme by applied magnetic field.

3.4.5. Crystallinity

Effects of xenon lamp irradiation and immobilization on the crystallinity were studied by XRD analysis. As seen from Fig. 10, crystalline phases of the immobilized enzyme were identical to those of poly(MAA)-decorated Fe_3O_4 as well as the freshly prepared Fe_3O_4. The six characteristic peaks occurred at 2θ of 30.1, 35.5, 43.2, 53.5, 57.0 and 62.8, represented corresponding indices (2 2 0); (3 1 1); (4 0 0); (4 2 2); (5 1 1) and (4 4 0), respectively, of Fe_3O_4. The result above revealed clearly that xenon lamp irradiation and immobilization did not result in phase change of Fe_3O_4 nanoparticles in the present case. However, we could not absolutely conclude that xenon lamp irradiation would not result in phase change or oxidation of Fe_3O_4. Changes in crystalline structure might be related to the irradiation time, irradiation intensity and atmosphere, etc.

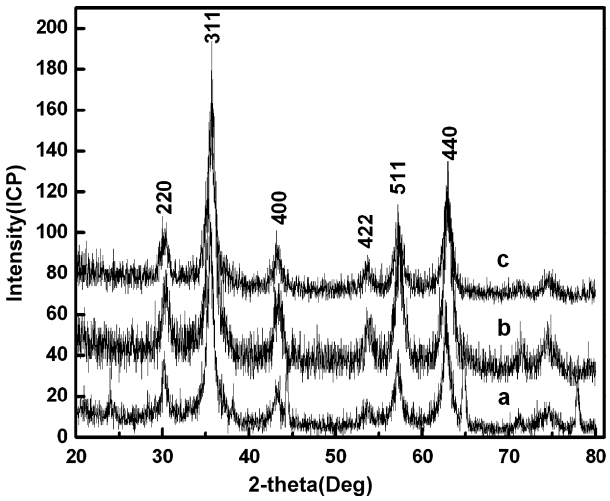

Fig. 10. Crystalline structures of (a) freshly prepared Fe_3O_4; (b) carboxyl-functionalized superparamagnetic nanogels; and (c) immobilized CT.

3.4.6. Enzyme activity

Enzyme immobilization was an important technique, which ensured recycling of the biocatalyst, permitted easy product separation and improved the performances of enzymes. In this sense, high enzyme activity was necessarily required for immobilized enzymes to improve the catalysis efficiency in practical applications. The activity of an immobilized enzyme depended on a number of factors, which could be summarized as size and shape of the carrier material, the nature of the immobilization method, the composition of the carrier material and the specific conditions during immobilization [28]. Herein, specific activity of the immobilized enzyme was determined to be 0.77 U/(mg min), a residual activity of 82.7% was retained for CT (0.93 U/(mg min)) after being bound to the support. The loss in enzyme activity might be arising from the conformational changes, steric hindrance and transfer limitation, etc.

4. Conclusion

In this paper, novel carboxyl-functionalized magnetic nanogels were prepared by facile photochemical in situ polymerization. CT as model enzyme was covalently conjugated onto the carboxyl-functionalized magnetic nanogels by EDC and NHS at room temperature. Enzyme immobilization led to marked change in particle size, as a result of aggregation of immobilized enzyme and linkage between magnetic particles. Irradiation and surface coating did not result in phase change of Fe_3O_4. Superparamagnetic properties were retained for Fe_3O_4 while slightly reducing its saturation magnetization in comparison to freshly prepared Fe_3O_4. The binding capacity was determined to be 30 mg enzyme/g nanogel and 37.5 mg enzyme/g nanogel by TG

analysis and BCA protein assay, respectively. Specific activity of the immobilized enzyme was calculated to be 0.77 U/(mg min), 82.7% as that of free counterpart. The immobilized enzyme was susceptive to external magnetic field, and could be expected to be used in the continuous system of biocatalysis in future.

Acknowledgments

The authors are grateful to financial supports from Shanghai Municipality Commission for Special Project of Nanometer Science and Technology (No. 0452nm068) and National Natural Science Foundation of China (20504010). Many thanks to Professor Li Yuan.

References

[1] C. Guarise, L. Pasquato, V. De Filippis, P. Scrimin, Proc. Natl. Acad. Sci. U.S.A. 103 (2006) 3978.
[2] F. Bellezza, A. Cipiciani, M.A. Quotadamo, Langmuir 21 (2005) 11099.
[3] M.I. Kim, H.O. Ham, S.D. Oh, H.G. Park, H.N. Chang, S.H. Choi, J. Mol. Catal. B: Enzym. 39 (2006) 62.
[4] J. Kim, J.W. Grate, Nano Lett. 3 (2003) 1219.
[5] A. Dyal, K. Loos, M. Noto, S.W. Chang, C. Spagnoli, K.V.P.M. Shafi, A. Ulman, M. Cowman, R.A. Gross, J. Am. Chem. Soc. 125 (2003) 1684.
[6] X.R. Zhai, W.Z. Wei, J.X. Zeng, X.Y. Liu, S.G. Gong, Anal. Lett. 39 (2006) 913.
[7] M.H. Liao, D.H. Chen, Biotechnol. Lett. 23 (2001) 1723.
[8] K. Nishimura, M. Hasegawa, Y. Ogura, T. Nishi, K. Kataoka, H. Handa, M. Abe, J. Appl. Phys. 91 (2002) 8555.
[9] L.M. Rossi, A.D. Quach, Z. Rosenzweig, Anal. Bioanal. Chem. 380 (2004) 606.
[10] F. Horst, E.H. Rueda, M.L. Ferreira, Enzyme Microb. Technol. 389 (2006) 1005.
[11] L. Zeng, K.K. Luo, Y.F. Gong, J. Mol. Catal. B: Enzym. 38 (2006) 24.
[12] D. Horák, B. Rittich, J. Šafář, A. Španová, J. Lenfeld, M.J. Beneš, Biotechnol. Prog. 17 (2001) 447.
[13] T. Bahar, S.S. Celebi, Enzyme Microb. Technol. 26 (2000) 28.
[14] B.R. Pieters, G. Bardeletti, Enzyme Microb. Technol. 14 (1992) 361.
[15] T.S. Yu, J.P. Lin, J.F. Xu, T. Chen, S.L. Lin, Polymer 46 (2005) 5695.
[16] X.J. Xu, L.M. Gan, Curr. Opin. Colloid Interface Sci. 10 (2005) 239.
[17] M.L. Luo, W. Tang, J.Q. Zhao, C.S. Pu, J. Mater. Process. Technol. 172 (2006) 431.
[18] A.J. Hoffman, G. Mills, H. Yee, M.R. Hoffmann, J. Phys. Chem. 96 (1992) 5546.
[19] A.L. Stroyuk, V.M. Granchak, A.V. Korzhak, S.Y. Kuchmii, J. Photochem. Photobiol. A: Chem. 162 (2004) 339.
[20] P.J. Gong, J.H. Yu, H.W. Sun, J. Hong, S.F. Zhao, D.M. Xu, S.D. Yao, J. Appl. Polym. Sci. 101 (2006) 1283.
[21] H.W. Sun, J.H. Yu, P.J. Gong, D.M. Xu, C.F. Zhang, S.D. Yao, J. Magn. Magn. Mater. 294 (2005) 273.
[22] S.C. Qu, H.B. Yang, D.W. Ren, S.H. Kan, G.T. Zou, D.M. Li, M.H. Li, J. Colloid Interface Sci. 215 (1999) 190.
[23] H.W. Sun, J. Hong, F.Z. Meng, P.J. Gong, J.H. Yu, Y.L. Xue, S.F. Zhao, D.M. Xu, L. Dong, S.D. Yao, Surf. Coat. Technol. 201 (2006) 250.
[24] X. Xie, X. Zhang, H. Zhang, D.P. Chen, W.Y. Fei, J. Magn. Magn. Mater. 277 (2004) 16.
[25] M. Mikhaylova, D.K. Kim, C.C. Berry, A. Zagorodni, M. Toprak, A.S.G. Curtis, M. Muhammed, Chem. Mater. 16 (2004) 2344.
[26] D.H. Chen, M.H. Liao, J. Mol. Catal. B: Enzym. 16 (2002) 283.
[27] D.K. Kim, Y. Zhang, W. Voit, K.V. Rao, M. Muhammed, J. Magn. Magn. Mater. 225 (2001) 30.
[28] E. Emregul, S. Sungur, U. Akbulut, Food Chem. 97 (2006) 591.